

PACS numbers: 42.55.Rz; 42.60.By; 42.60.Jf
DOI: 10.1070/QE2015v045n05ABEH015770

Front-end system for Yb:YAG cryogenic disk laser

E.A. Perevezentsev, I.B. Mukhin, I.I. Kuznetsov, O.L. Vadimova, O.V. Palashov

Abstract. **A new front-end system for a cryogenic Yb:YAG laser is designed. The system consists of a femtosecond source, a stretcher and a regenerative amplifier with an output energy of 25 μJ at a pulse repetition rate of 49 kHz, a pulse duration of ~2 ns and a bandwidth of ~1.5 nm. After increasing the pump power of the regenerative amplifier, it is expected to achieve a pulse energy of ~1 mJ at the input to cryogenic amplification stages, which will allow one to obtain laser pulses with a duration of several picoseconds at the output of the cryogenic laser after compression.**

Keywords: *pulsed laser, disk laser, Yb:YAG, regenerative amplifier, Bragg gratings, diffraction gratings.*

1. Introduction

Researchers of the Institute of Applied Physics, Russian Academy of Sciences, work on the creation of a repetitively pulsed laser with a high pulse energy (~1 J) at a high pulse repetition rate (~1 kHz) [1]. High-power amplification stages are based on thin-disk Yb:YAG active elements (AEs) cooled to liquid nitrogen temperature. These technologies allow one to improve heat removal from the AE, decrease the thermally induced distortions and increase the amplification efficiency. A front-end system for these cryogenic amplifiers was developed by us based on an Yb:YAG disk with water cooling and the following output parameters: pulse repetition rate 1–2 kHz, pulse energy ~1 mJ and pulse duration 3–7 ns, which was obtained using *Q*-switching by a Pockels cell [1]. One of the main applications of high-energy systems with a high pulse repetition rate is pumping of parametric amplifiers of broadband femtosecond lasers [2, 3]. This requires shortening of pump pulses to a few picoseconds and precise matching of the amplified and pump pulses. The best matching is achieved in a scheme in which a master oscillator for both the femtosecond and pump channels is a broadband femtosecond laser. In addition, this source allows pumping with a needed duration. To implement the above concept, we purchased an Antaus (Avesta) laser system consisting of a fibre femtosecond laser with an amplifier and the following output characteristics: pulse energy 1 μJ, pulse duration 200 fs, bandwidth 8 nm and pulse repetition rate 3 MHz. The radiation of this source is divided into two (signal and pump) channels. In the future, we plan to compress the signal pulse to a duration of ~20 fs in a commercial gas compressor and to stretch it by chirped mirrors to a duration of ~10 ps. In the present work, we consider the pump channel, which is used as a base for producing a new front-end laser system for a cryogenic disk amplifier.

E.A. Perevezentsev, I.B. Mukhin, I.I. Kuznetsov, O.L. Vadimova, O.V. Palashov Institute of Applied Physics, Russian Academy of Sciences, ul. Ul'yanova 46, 603950 Nizhnii Novgorod, Russia; e-mail: palashov@appl.sci-nnov.ru, mib_1982@mail.ru, eperevezentsev@gmail.com, ivanushka911@yandex.ru, musfex@mail.ru

Received 29 January 2015; revision received 10 February 2015
Kvantovaya Elektronika **45** (5) 451–454 (2015)
Translated by M.N. Basieva

2. Stretcher of the front-end system

According to experimental results, amplification in cryogenic stages occurs without distortions in the case of pulses with a spectral width at half maximum of ~0.7 nm, which corresponds to a transform-limited pulse duration of ~2 ps [1]. For calculating the stretcher parameters, the total radiation bandwidth $\Delta\lambda$ was determined to be 1.5 nm at a level of 0.03. To stretch such a narrow-band pulse in time to 1 ns, the group delay dispersion of the stretcher material must be high, which considerably restricts the choice of an appropriate optical element.

2.1. Stretcher based on holographic diffraction gratings

In the first experiments, we used an available holographic diffraction grating (DG) with dimensions of 32 × 24 cm and a groove density of 1200 grooves mm^{-1}. Usually, a stretcher consists of a pair of DGs separated by an optical system with a magnification of –1 [4]. Such an optical system forms in the image domain a 'virtual compressor', which consists of a pair of parallel DGs, namely, of the second grating of the stretcher and the image of the first grating [5–7]. In this case, the absolute values of the dispersion of all orders are precisely matched (identical in absolute values but opposite in signs) to the dispersion of a Treacy compressor [4] provided that the line densities and the angles of light incidence on the grating coincide. Thus, to design a stretcher, we at first calculated the parameters of the future compressor [8–10].We ascertained that the dimensions of the available DG are sufficiently large. As an optical system with a magnification of –1, we chose a 2*Nf* optical system [11, 12] (or equivalent). This system consists of two confocal positive lenses with identical focal distances f and a collecting lens in their common focus. The focal distance of the negative collecting lens is determined as $f_{col} = f/[2(N-2)]$. In practice, one most often uses a Martinez optical system with a plane collecting mirror, $N = 2$ [7, 4], or the Öffner 6*f* optical system with a convex collecting mirror, $N = 3$ [13–19]. For us, the N parameter was free and allowed us to calculate and assemble a rather small-size (120 × 100 cm) stretcher with a required dispersion; in our scheme, we use $N = 7$.

The experimental scheme is shown in Fig. 1. The radiation of a femtosecond master oscillator propagates through a Faraday isolator, after which the pulse repetition rate decreases by a Pockels cell (PC) based on a BBO crystal (EKSMA, Lithuania), and the beam enters the stretcher. The output beam spectrum and temporal profile are presented in Fig. 2. One can see that these characteristics satisfy our requirements. The main drawback of the stretcher was that the angle of incidence of the beam on the DG (α = 15°) strongly differed from the Littrow angle (θ_L = 38°), which led to high losses (only about 10% of energy passed through the stretcher). The optimisation calculation presented below showed that, using a standard DG with a groove density of 1740 grooves mm^{-1}, it is possible to decrease the DG width from 32 to 24 cm and work at an angle of incidence close to the Littrow angle, i.e., with minimal losses. In addition, the closer the N parameter to three, the lower the aberrations. In the optimal scheme, N = 4.

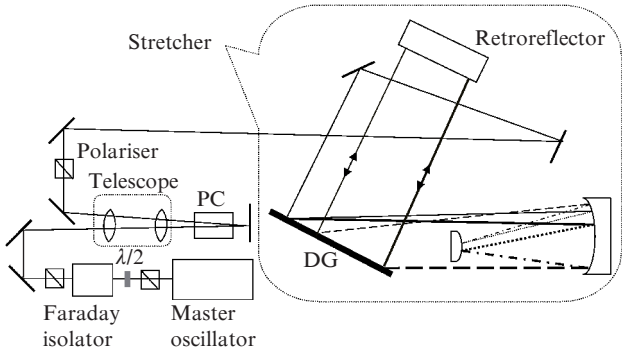

Figure 1. Scheme of a stretcher based on a holographic DG; thin lines correspond to the long-wavelength edge of the spectrum, and thick lines correspond to the short-wavelength edge.

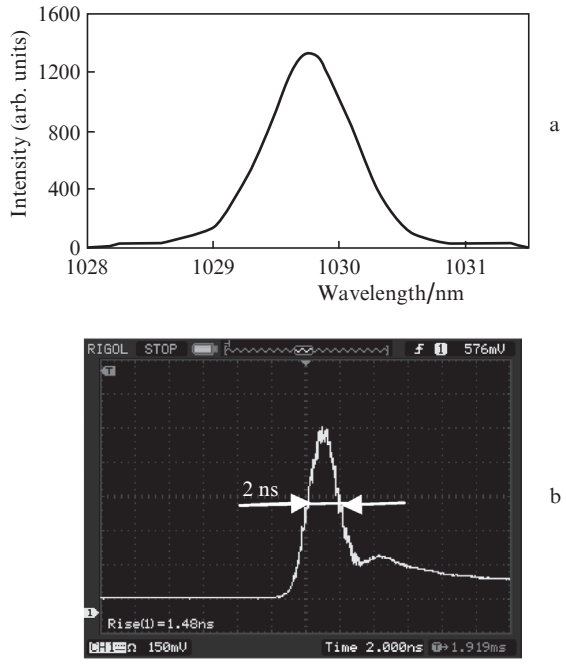

Figure 2. (a) Spectrum and (b) time profile of radiation pulses at the exit of a stretcher based on a holographic DG.

2.2. Stretcher based on chirped volume Bragg gratings

In recent years, the technologies of production of one more type of dispersive elements – chirped volume Bragg grating (CVBG) – have been extensively developed and upgraded. The principle of operation of CVBGs is similar to the principle of operation of chirped mirrors, but the incoming phase difference between the short- and long-wavelength beams in the case of CVBGs is several orders of magnitude higher. CVBGs are not as universal as holographic DGs, but have some advantages, namely, they are easy to adjust, are compact, can provide both positive and negative group delay dispersions, etc. Until recently, commercially available CVBGs had a maximum stretching factor of 100 ps nm^{-1} per reflection, i.e., at a pulse bandwidth of 0.7 nm, one had to use more than 15 reflections. Taking into account that the angle of incidence on a CVBG is assigned and each grating is rather expensive, it was difficult to produce a stretcher based on these gratings. However, recently commercially available CVBGs from OptiGrate with a high time-stretch factor per reflection have been reported [20]. We purchased two gratings with a time-stretch factor of 220 ps nm^{-1} at a spectral width of 2.2 nm. The reflection maximum lied at the desired wavelength 1029.7 nm at the angle of incidence on the grating of 5°. Using polarisation decoupling methods, we assembled a compact stretcher with four reflections from each grating (Fig. 3). At the output, we obtained 2-ns pulses with a bandwidth of ~1.5 nm, which corresponds to the required parameters (Fig. 4). The losses in the spectral range of interest were ~50%.

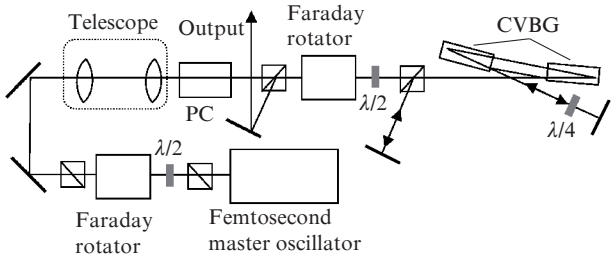

Figure 3. Scheme of a CVBG stretcher.

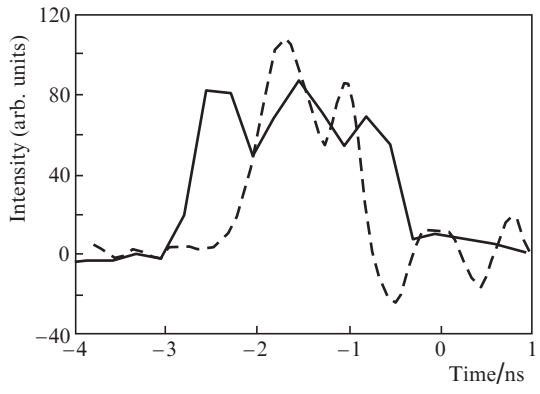

Figure 4. Time profiles of pulses at the exit of a CVBG stretcher (solid curve) and at the output of a regenerative amplifier (dashed curve).

3. Regenerative amplifier

One of the optical synchronisation problems is that one has to amplify the pump signal energy from a submicrojoule level to several joules. To amplify a signal by several orders of magnitude, it is proposed to use a thin-rod amplifier after the stretcher [21]. Thin-rod AEs can have a gain of 10–30 and provide an output pulse energy exceeding 1 mJ, which is more than enough for an input signal of a cryogenic disk laser.

A thin Yb:YAG rod (dopant concentration 1%) 1.2 mm in diameter and 30 mm long is used in the single-crystal fibre geometry (Fig. 5). The pump radiation is coupled in through two faces and propagates through the crystal multiply reflecting from its side surface due to the total internal reflection. The signal radiation is coupled in through dichroic mirrors and easily passes through the AE crystal without touching its lateral side. The rod was cooled from the lateral side, for which purpose it was mounted in a copper heat sink using indium solder as an intermediate material. The heat sink was cooled by running water flowing in its internal channels.

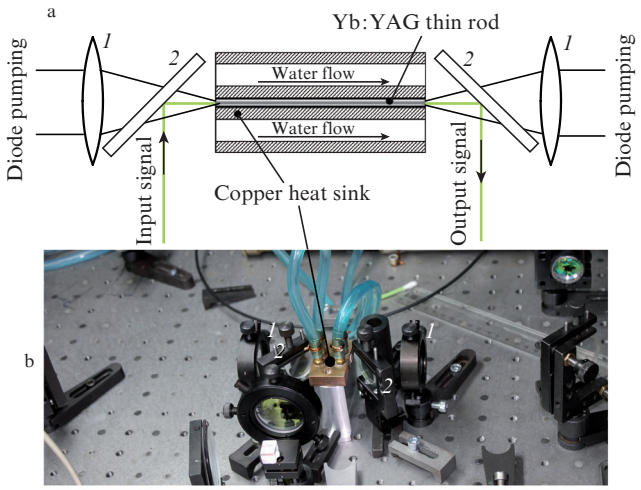

Figure 5. (a) Cooling and pumping scheme of a thin Yb:YAG rod and (b) a photograph of a thin-rod laser head.

The small-signal gain in the developed thin-rod laser head was measured as a function of pump power (Fig. 6). The maximum gain per pass was only two times, which relates to a low pump power. Indeed, the gain in an AE begins to exceed unity at an absorbed pump power of 30 W, which completely corresponds both to calculations and to the results of works [21, 22]. Note that the gain is almost the same for pulsed and cw pumping, which indicates the absence of thermal effects. To achieve the desired tenfold gain per pass, one must increase the pump power approximately by a factor of 2.5 and decrease the AE diameter from 1.2 to 1 mm. By using such an AE in an ordinary four-pass scheme, the signal after the stretcher of the front-end system will be amplified by about 10^4 times (to 1 mJ). The pulse repetition rate in this case can be 1–20 kHz with the same pulse energy.

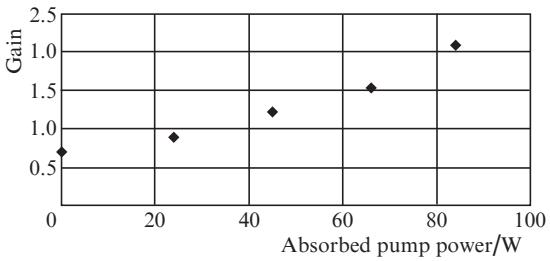

Figure 6. Small-signal gain in a thin rod under cw pumping.

To achieve a required gain, one can use a regenerative amplifier. Despite some drawbacks (poor contrast and insufficient stability) compared to multipass amplifiers, it is the regenerative amplification principle that is most often used to significantly increase the pulse energy of fibre sources.

Based on a thin-rod AE, we fabricated a regenerative amplifier according to the scheme shown in Fig. 7. For the laser head described above, we assembled a cavity with one of the shoulders increased to 0.7 m with the help of of a telescopic system consisting of a negative lens and a concave mirror. The cavity includes a polariser and a Pockels cell for coupling the amplified radiation in and out. This cavity was adjusted for stable lasing of single-mode radiation with an output power up to 4 W at the maximum pump power. Note that the main drawback of the thin-rod AE geometry is the appearance of a strong thermal lens (its focal distance in the studied AE was ~0.5 m). This leads to the necessity of readjusting the telescopic shoulder of the cavity with changing the pump power.

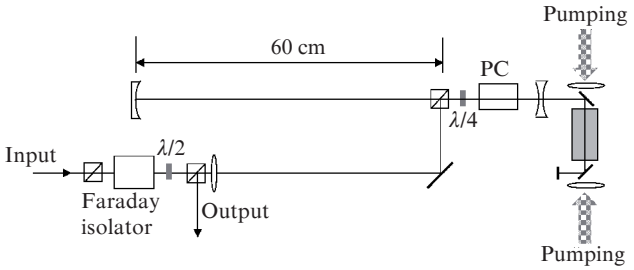

Figure 7. Scheme of a thin-rod regenerative amplifier.

In the regenerative amplification regime, the beam after the stretcher is focused by a lens to form the input signal divergence corresponding to the divergence of the cavity mode. Then, one of the pulses is blocked in the cavity by applying voltage to the Pockels cell synchronised with the femtosecond source via the control unit. The number of amplification passes is measured by a photodiode placed behind the highly reflecting mirror and can be controlled by the delay in switching off the Pockels cell. After the second switching action, the amplified pulse returns and is coupled out by a Faraday isolator placed behind the stretcher.

In the developed regenerative amplification scheme, we managed to amplify the pulse energy after the stretcher from 0.1 to 25 μJ per 15 cavity round trips. In this case, the pulse repetition rate was 49 kHz at an average output power of 1.3 W. The amplified pulse becomes slightly shorter than the pulse after the stretcher since the pulse is cut by the Pockels cell due to insufficient length of the telescopic shoulder of the cavity (see Fig. 4, which presents an oscillogram of an amplified pulse recorded by a photodiode with a response time of 70 ps and an oscilloscope with a transmission band of 2.5 GHz). Note also that the amplified pulse profile is close to

the Π-shaped profile of the pulse after the stretcher. The retention of this pulse profile is very important for further amplification in a cryogenic disk laser because the pump pulse profile determines the parametric amplification efficiency.

Note that it is planned to increase the gain, which was 250 in the developed regenerative amplifier, to 10^4. The main factor restricting the gain is high loss at the polariser due to depolarisation arising in the AE and the Pockels cell. Due to this loss, it is necessary to increase the number of passes through the amplifier, which, in turn, is limited by the beginning of a 'continuous' lasing regime (beginning of giant pulse generation). The depolarisation in the AE can be compensated for by a quarter-wave plate placed between the AE and the highly reflecting mirror of the cavity, while the depolarisation in the Pockels cell, which is obviously caused by its position in the diverging beam, can be decreased by its replacement to the region of better beam collimation.

4. Conclusions

To develop a stretcher needed for the new front-end system, it is reasonable to use both holographic DGs and CVBGs because they have a high dispersion. In the course of the study, we designed a program for numerical simulation of the paths of beams in various equivalent one- and two-grating stretcher schemes at given parameters of a future grating compressor. A scheme of a stretcher based on DGs with a groove density of 1200 grooves mm^{-1} is calculated and experimentally implemented. The parameters of optical elements and DGs needed for the development of a more optimal (from the viewpoint of transmission, dimensions and cost) stretcher are determined. According to calculations, when a grating with a groove density of 1740 grooves mm^{-1} is used, its width decreases from 32 to 24 cm, and the working angle of incidence becomes close to the Littrow angle, which leads to an increase in the first-order diffraction efficiency. A stretcher based on two CVBGs with four reflections from each grating is experimentally implemented. The developed scheme is much more compact than the previous one and is simpler aligned.

A laser head based on a thin Yb:YAG rod (dopant concentration 1%) 1.2 mm in diameter and 30 mm in length is developed in the single-crystal fibre geometry. Based on this laser head, we produced a regenerative amplifier, which allowed us to amplify the energy of pulses after the stretcher from 0.1 to 25 μJ per 15 cavity roundtrips. In this case, the pulse repetition rate was 49 kHz at an average output power of 1.3 W. It is expected to increase the gain from obtained 250 to 10^4 by increasing the pump power.

Thus, we have developed a new front-end system for a cryogenic disk laser, which consists of a femtosecond source, a stretcher and a regenerative amplifier. After increasing the pump power of the regenerative amplifier, the output radiation of the front-end system will be amplified in cryogenic amplification stages.

Acknowledgements. This work was supported by the Presidium of the Russian Academy of Sciences (Extreme Light Fields and Their Applications Programme). The element base was created using funds of Megagrant No. 14.B25.31.0024 of the Government of Russian Federation, awarded to the Institute of Applied Physics, Russian Academy of Sciences.

References

1. Perevezentsev E.A., Mukhin I.B., Kuznetsov I.I., Vadimova O.L., Palashov O.V. *Kvantovaya Elektron.*, **44** (5), 448 (2014) [*Quantum Electron.*, **44** (5), 448 (2014)].
2. Brown D.C., Tornegård S., Kowalewski K., Envid V., Zembek J. *Proc. SPIE Int. Soc. Opt. Eng.*, **8381**, 83810R-1 (2012).
3. Klingebiel S., Wandt C., Skrobol C., Ahmad I., Trushin S.A., Major Z., Krausz F., Karsch S. *Opt. Express*, **19** (6), 5357 (2011).
4. Martinez O.E. *IEEE J. Quantum Electron.*, **QE-23** (1), 59 (1987).
5. Treacy E.B. *IEEE J. Quantum Electron.*, **QE-5** (9), 454 (1969).
6. Naik P.A., Sharma A.K. *J. Opt. (Calcutta)*, **29** (3), 105 (2000).
7. Fiorini C., Sauteret C., Rouyer C., Blanchot N., Seznec S., Migus A. *IEEE J. Quantum Electron.*, **30** (7), 1662 (1994).
8. Cheriaux G. *Thes. Doct.* (Orsay, Universite Paris XI, 1997).
9. Yakovlev I.V. *Osobennosti sistemy stretcher–kompressor dlya parametricheskikh usilitelei chirpirovannykh impul'sov s preobrazovaniem chastoty* (Specific Features of a Stretcher–Compressor System for Parametric Amplifiers of Chirped Pulses with Frequency Conversion) (N. Novgorod: IPF RAN, 2013).
10. McMullen J.D. *Appl. Opt.*, **18** (5), 737 (1979).
11. Gitin A.V. *Kvantovaya Elektron.*, **38** (11), 1021 (2008) [*Quantum Electron.*, **38** (11), 1021 (2008)].
12. Zhang Z., Yagi T., Arisawa T. *Appl. Opt.*, **36**, 3393 (1997).
13. Ross I.N., Langley A.J., Today P. *Central Laser Facility Annual Report*, 1999/2000, p. 201.
14. Collier J., Hernandez-Gomez C. *Central Laser Facility Annual Report*, 2001/2002, p. 173.
15. Cheriaux G., Walker B., Dimauro L.F., Rousseau P., Salin F., Chambaret J.P. *Opt. Lett.*, **21**, 414 (1996).
16. Öffner A. Patent 3 748 015 US (1971).
17. Jiang J., Zhang Z., Hasama T. *J. Opt. Soc. Am. B*, **19**, 678 (2002).
18. Zhang Z., Song Y., Sun D., Chai L., Sun H., Wang C. *Opt. Commun.*, **206** (1), 7 (2002).
19. Suzuki A. *Appl. Opt.*, **22**, 3943 (1983).
20. Glebov L., Smirnov V., Rotari E., Cohanoschi I., Glebova L., Smolski O., Lumeau J., Lantigua C., Glebov A. *Opt. Eng.*, **53** (5), 051514 (2014).
21. Délen X., Piehler S., Didierjean J., Aubry N., Voss A., Ahmed M.A., Graf T., Balembois F., Georges P. *Opt. Lett.*, **37** (14), 2898 (2012).
22. Zaouter Y., Martial I., Aubry N., Didierjean J., Hönninger C., Mottay E., Druon F., Georges P., Balembois F. *Opt. Lett.*, **36** (5), 748 (2011).